Molecular Therapy
Nucleic Acids
Original Article

CHD6 eviction of promoter nucleosomes maintains housekeeping transcriptional program in prostate cancer

Lina Bu,[1,2,5] Shaodong Huang,[1,2,5] Ziyan Rao,[1,2] Chenyang Wu,[1,2] Bryan-Yu Sun,[1] Yanhua Liu,[3,4] Lin He,[3,4] and Dongyu Zhao[1,2]

[1]Department of Biomedical Informatics, School of Basic Medical Sciences, Peking University, Beijing 100191, China; [2]State Key Laboratory of Vascular Homeostasis and Remodeling, Peking University, Beijing 100191, China; [3]Department of Integration of Chinese and Western Medicine, School of Basic Medical Sciences, Peking University, Beijing 100191, China; [4]Department of Biochemistry and Molecular Biology, School of Basic Medical Sciences, Peking University, Beijing 100191, China

CHD6, a member of the chromodomain helicase DNA-binding protein family, has been implicated in various diseases and tumors. However, its precise binding model of CHD6 on regulatory functional genes remains poorly understood. In this study, we discovered sharp peaks of CHD6, as the first member of CHD family for housekeeping process, binding only to the promoter region of genes in the C4-2 cell line. These genes, with conserved sharp CHD6 peaks across tumor cells, likely represent housekeeping genes *ADNP* and *GOLGA5*. Genes with sharp CHD6 peaks exhibit stable and low expression levels, sharing epigenetic features similar to housekeeping genes. Furthermore, this regulatory model also exists in both HEK293 cells and cardiomyocytes. Overall, the results of this study demonstrate that CHD6 binds to the promoter regions of housekeeping genes, regulating their histone modifications, chromatin structure, and gene expression.

INTRODUCTION

Prostate cancer (PC) is one of the most widespread malignancies in men worldwide, with an estimated 1,466,718 new cases diagnosed globally in 2024.[1] Despite multiple available treatment options, including active surveillance, chemotherapy, radiation therapy, hormone therapy, surgery, and cryotherapy, PC remains incurable.[2] As time progresses, this disease continues to develop resistance to various conventional treatment approaches.[3] Castration-resistant prostate cancer (CRPC) is considered incurable.[4] Thus, there is an urgent need to identify more molecular biomarkers for CRPC. In addition, investigating the molecular mechanisms underlying CRPC progression is critical and may help provide new therapeutic targets. Chromatin remodelers are pivotal in regulating chromatin accessibility and nucleosome positioning on genomic DNA, which is essential for all DNA-dependent biological processes.[5,6] Recent research has indicated that chromatin remodelers are involved in both human cancer and neurological disorders, offering insights into new mechanisms and potential therapeutic avenues.[7–9]

As a member of the chromatin remodeling factor family, the chromodomain helicase DNA-binding protein (CHD) family includes nine members, CHD1–CHD9.[10] These members share double chromodomains for binding specifically modified histones[11–13] and an SNF2-like ATP-dependent helicase domain that alters chromatin packaging.[14] They are considered crucial factors in establishing the nucleosome landscape essential for oncogenes (OGs), tumor suppressor genes (TSGs), and housekeeping (HK) genes, thereby controlling fundamental processes, including transcription, proliferation, and epigenetic perturbation.[15] The emerging dysregulation of CHD in various human cancers emphasizes the vital significance of chromatin dynamics in tumorigenesis.[16–20] CHD6, belonging to the subfamily III of CHD, is expressed ubiquitously in mammalian tissues. CHD6 plays a crucial role in and has associations with multiple diseases. Previous reports have highlighted the significant involvement of CHD6 in DNA damage and repair and autophagy.[21,22] CHD6 collaborates with TCF4 to positively regulate *TMEM65* gene expression, thereby promoting colorectal cancer development and metastasis.[23] Meanwhile, CHD6 binds on chromatin to evict nucleosomes from promoters and gene bodies for transcriptional activation in PC.[24] HK, developmental, and OG transcriptional programs are highly regulated to maintain cell identity and function. The involvement of CHD6 in the regulation of HK genes and how it impacts the chromatin structure of these genes remains unclear, despite CHD6 being a cancer driver gene.

HK genes are often assumed to be stably expressed and essential for the maintenance of basal cellular processes, which ensures the essential functions for cell survival across various tissues or organisms.[25,26] However, evidence indicates that HK genes may vary in expression levels under diverse experimental conditions.[27–29] Despite their common use as internal reference genes for gene expression assessment, changes in their expression levels have been associated with cancer development.[30] A study focused on prostate tumorigenesis revealed

Received 16 July 2024; accepted 13 November 2024;
https://doi.org/10.1016/j.omtn.2024.102397.

[5]These authors contributed equally

Correspondence: Dongyu Zhao, Department of Biomedical Informatics, School of Basic Medical Sciences, Peking University, Beijing 100191, China
E-mail: zhao.dongyu@pku.edu.cn

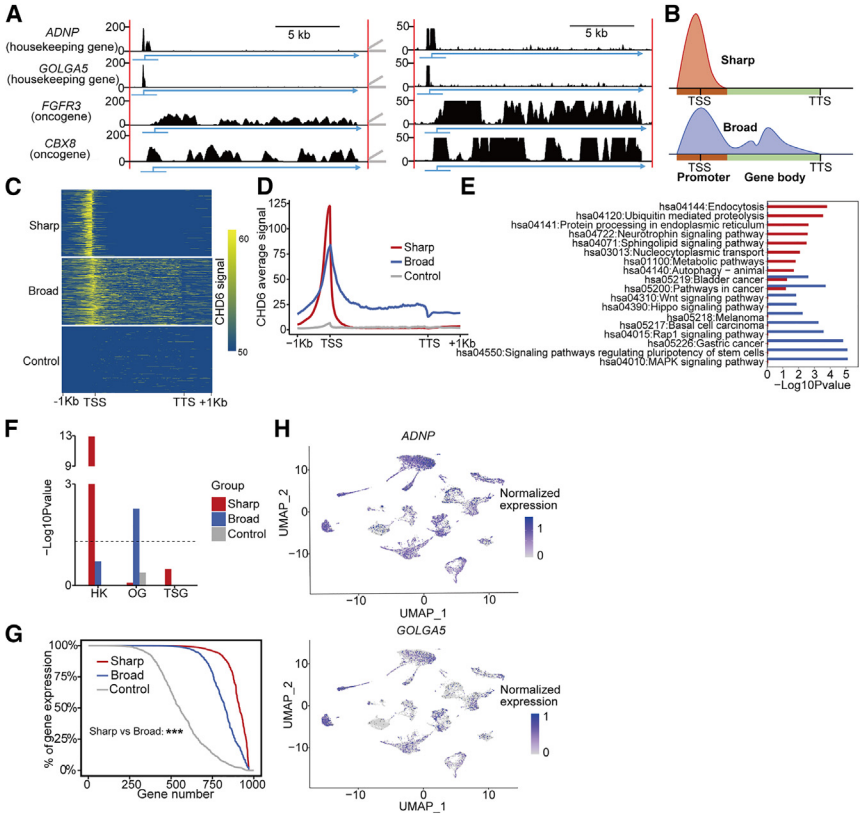

Figure 1. Sharp CHD6 peaks in the C4-2 cell line

(A) Density of CHD6 in the housekeeping (HK) genes *ANDP* and *GOLGA5* and the oncogenes (OGs) *FGFR3* and *CBX8*. (B) Definition of genes with sharp and broad CHD6 peaks. (C) Heatmap of CHD6. Each row represents a gene region from −1 to +1 kb with respect to the gene. Top: the top 1,000 sharp CHD6 peaks; center: the top 1,000 broad CHD6 peaks; bottom: 1,000 random genes. (D) Average ChIP-seq signal value of CHD6 plotted around groups. (E) KEGG pathway enrichment of genes with sharp, broad, and control peaks. (F) Enrichment *p* values (y axis) of HK genes, OGs, and tumor suppressor genes (TSGs) in the different groups. (G) The percentage of gene expression. (H) Expression levels of the HK genes *ANDP* and *GOLGA5* in tumor and normal cells. For (F), *p* values determined using Fisher's exact test. For (G), *p* values determined using one-tailed Wilcoxon test. $^{*}p < 0.05$; $^{**}p < 0.01$; $^{***}p < 0.001$.

that HK genes were more likely differentially expressed, hinting at their potential role in driving cancer development. Another study suggested that the variable expression levels of HK genes can act as diagnostic and prognostic indicators in lung cancers.[31] While cancer development induced by HK genes expressions has been reported previously, the mechanisms by which chromatin remodelers regulate their expression levels and affect their epigenetic modifications remain poorly understood.

In this study, to gain insights into how the binding models of CHD6 influence the expression levels and epigenetic modifications of distinct functional genes, we conducted a comprehensive analysis using multi-omics approaches on prostate cancer cells. We found that genes associated with sharp CHD6 peaks are enriched in HK genes rather than cancer-related genes. It is interesting that this model is consistent across normal human cells.

RESULTS

Sharp enrichment of CHD6 at promoter region of HK genes in cancer cells

Our previous study demonstrated that CHD6 binds on chromatin to evict nucleosomes from promoters and gene bodies, which leads to the transcriptional activation of oncogenic pathways.[24] However, previous research has not clearly elucidated how the distinct binding regions of CHD6 influence transcriptional programs. To assess the direct regulatory regions of CHD6, we analyzed the distribution of all peaks across the genome, from transcription start site (TSS) to transcription termination site (TTS), using CHD6 chromatin immunoprecipitation sequencing (ChIP-seq). Among the total peaks, a notable enrichment of promoters and gene bodies is shown in a pie chart (Figure S1A). To gain further insight into how CHD6 regulates gene expression levels, we recently observed the CHD6 signal and found that it bound to the promoter region (±1 kb of TSS) of several well-known HK genes,[25] such as *ADNP* and *GOLGA5*, in the C4-2 cell line (Figure 1A). By contrast, CHD6 covered low-density genetic regions, from promoters to gene bodies, on OGs such as *FGFR3* and *CBX8* (Figure 1A). This observation motivated us to perform a systematic analysis of the regions (promoters and gene bodies) associated with each CHD6 peak. We observed a subset of high-density CHD6 peaks on relatively narrow promoters (defined as sharp CHD6 peaks) and a subset of low-density CHD6 peaks that were exceptionally wide (defined as broad CHD6 peaks), spanning both the promoter and gene body regions (Figure 1B). We found no overlap between the sharp and broad peaks, which suggests potentially distinct mechanisms for these two groups of peaks. To conduct a quantitative comparison of sharp and broad CHD6 peaks, we retrieved 1,000 genes associated with sharp and broad CHD6 peaks based on the total signal of CHD6 and randomly chose another 1,000 genes as control (Figure 1C). Distinct CHD6 binding signals were found only in the promoter region on sharp CHD6 peaks, whereas the entire gene exhibited CHD6 binding signals on broad CHD6 peaks (Figure 1D). As expected, the signal density of the sharp CHD6 peaks was higher than that of the broad and control CHD6 peaks in the promoter region.

We used Kyoto Encyclopedia of Genes and Genomes (KEGG) pathway analysis to characterize enriched functions of the genes

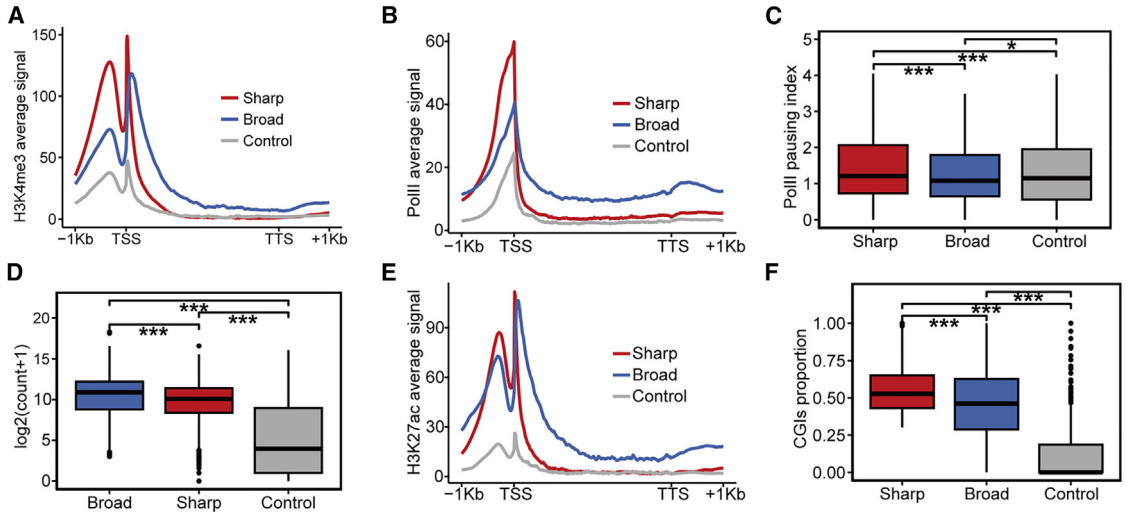

Figure 2. Epigenetic features of genes with sharp CHD6 peaks

(A) Average ChIP-seq signal value of H3K4me3 plotted around groups. (B) Average ChIP-seq signal value of RNA Pol II plotted around groups. (C) RNA Pol II pausing index plotted against sharp, broad, and control CHD6 peaks. (D) Boxplots showing gene expression levels (y axis) of the genes (n = 1,000 for each group), with the center line indicating the median. (E) Average ChIP-seq signal value of H3K27ac plotted around groups. (F) Boxplot showing CGI proportion (y axis) of groups. p values determined using one-tailed Wilcoxon test. *$p < 0.05$; **$p < 0.01$; ***$p < 0.001$.

associated with the three groups of CHD6 peaks. Endocytosis[32] (hsa04144) and autophagy[33] (hsa04140) were explicitly enriched in the group with sharp CHD6 peaks but not in the groups with broad or control CHD6 peaks (Figure 1E). This observation suggests that sharp CHD6 peaks might be associated with genes maintaining the HK process. By contrast, the Wnt signaling pathway[34] (hsa04310) is uniquely enriched in broad CHD6 peaks (Figure 1E). Pathways in cancer (hsa05200), referring to well-curated signaling networks involved in cancer development, were also significantly enriched in broad CHD6 peaks but not in the groups with sharp or control peaks (Figure 1E). To further confirm the association between sharp CHD6 peaks and the HK process, we collected high-confidence HK genes,[25] TSGs, and OGs (https://cancer.sanger.ac.uk/cosmic). We confirmed that this enrichment preference for HK genes was not due to bias in our driver gene collection, as TSGs and OGs showed similarly significant enrichment for the KEGG pathway in endocytosis (hsa04144) (Figure S1B), and OGs showed similarly significant enrichment for the KEGG pathway in autophagy animal (hsa04140) (Figure S1B). Surprisingly, the CHD6 group with the sharp peaks in the promoter region was enriched in HK genes but not in OG or TSG genes (Figure 1F).

We next analyzed the percentage of gene expression across different groups using the genotype-tissue expression (GTEx) tissue dataset and found that genes with sharp CHD6 peaks showed a universal expression compared with other genes (Figure 1G). We also used the single-cell RNA-seq (scRNA-seq) of 21,762 cells from 6 patients with CRPC using the 10X Genomics platform (Table S1). Analysis of the scRNA-seq data using CopyKAT resulted in the identification of aneuploid tumor and diploid normal cells in all six patients (Figure S1C). We found that genes with sharp CHD6 peaks, such as *ANDP* and *GOLGA5*, were expressed in all cells (Figure 1H), whereas genes with broad CHD6 peaks, such as *FGFR3* and *CBX8*, were expressed in only a few tumor cells (Figure S1D). Taking these data together, we conclude that sharp CHD6 peaks in the C4-2 cell line are strongly and uniquely associated with HK genes.

Sharp CHD6 genes have epigenetic signatures similar to those of HK genes

The enrichment level of histone H3 lysine 4 trimethylation (H3K4me3) at the initiation site of transcription, a hallmark of active gene promoters, is closely associated with gene expression level.[35,36] The latest research findings have indicated that H3K4me3 regulates RNA polymerase II (RNA Pol II) promoter-proximal pause-release and transcriptional elongation.[37,38] To understand the potential mechanisms underlying the sharp CHD6 peaks of genes, we mapped the ChIP-seq data of H3K4me3 and RNA Pol II in C4-2 cell line in three groups. The H3K4me3 and RNA Pol II ChIP-seq signals were more enriched in promoter regions of the genes with sharp CHD6 peaks than in those of the other genes (Figures 2A and 2B). This pattern of narrow H3K4me3 has been identified in the promoter regions of HK genes in several studies.[39–41] Furthermore, we observed that broad H3K4me3 (spanning over 4 kb) was enriched in the genes with broad CHD6 peaks but not in those with sharp peaks (Figure S2A). Given that the pausing index is the promoter-to-gene body ratio of RNA Pol II ChIP-seq density, a higher pausing index indicates more poised RNA Pol II and less elongation. Genes with sharp CHD6 peaks exhibited a higher RNA Pol II pausing index than other genes (Figure 2C), indicating that genes with sharp CHD6 peaks are in a state of promoter-proximal pausing. A previous study has shown that the promoter pausing of RNA Pol II plays a critical role in regulating HK genes.[42] Consistent with this observation, the

elongation-associated histone mark trimethylation of histone H3 at lysine 36 (H3K36me3)[43,44] showed weak signals in the genes with sharp CHD6 peaks (Figure S2B). In addition, we demonstrated that sharp CHD6 peaks were associated with expression levels significantly lower than those of genes with broad CHD6 peaks (Figure 2D). These results indicate that genes with sharp CHD6 exhibit epigenetic characteristics that are more similar to those of HK genes.

Common enhancers are generally believed to be involved in the transcription of HK genes.[45,46] Acetylation of histone H3 at lysine 27 (H3K27ac), an enhancer-associated mark, showed lower enrichment in the genes with sharp CHD6 peaks than in those with broad peaks (Figure 2E). Multiple adjacent enhancer elements can be clustered into super-enhancers (SEs), which are the major drivers of transcriptional activation.[47] In our analysis of ChIP-seq data on H3K27ac, we identified 1,121 SE genes. Similarly, genes with sharp CHD6 peaks did not display significant enrichment in SE genes, whereas the genes with broad peaks showed significant enrichment (Figure S2C). Another enhancer-associated mark, H3K4me1, also showed a lower signal in the genes with sharp CHD6 peaks than in those with broad peaks (Figure S2D), which aligns with the H3K27ac results. Moreover, using assay for transposase accessible chromatin sequencing to evaluate genome-wide chromatin accessibility, we observed that the genes with sharp CHD6 peaks exhibited lower chromatin accessibility than the genes with broad CHD6 peaks (Figure S2E).

H3K4me3 displayed a robust correlation with the boundaries of promoter-linked CpG islands (CGIs), and HK genes tended to have high CpG density.[48,49] Therefore, we compared the proportion of CGIs in the promoters of sharp and broad peaks and found a significantly higher proportion of CGIs on the genes with sharp CHD6 peaks than on the genes with broad and control peaks (Figure 2F). The results further revealed that the genes with sharp CHD6 peaks, such as HK genes, are enriched with CGIs in the promoter regions.

Genes with sharp CHD6 peaks show low but stable expression levels

To assess gene expression stability, we calculated the coefficient of variation (CV) and expression levels of genes across different groups using the GTEx tissue dataset. The CV of the genes with sharp CHD6 peaks was significantly lower than that of other genes (Figure 3A). Moreover, we observed significant decreases in the expression levels of genes with sharp CHD6 peaks compared with those with broad CHD6 peaks (Figure S3A). These expression patterns resembled those of HK genes, which are characterized by low but stable expression levels.[50] Therefore, our findings suggest that genes with sharp CHD6 peaks and HK genes share similar expression characteristics.

Given that CHD6 is an ATPase-dependent nucleosome remodeler that influences gene expression levels, we reasoned that CHD6 depletion might alter the occupancy of nucleosome at CHD6 binding sites. To map nucleosome occupancy on chromatin, we used micrococcal nuclease digestion with deep sequencing (MNase-seq) in both the C4-2 control and CHD6 knockdown cells. The occupancy of nucleosomes was higher in the genes with sharp peaks than in those with broad CHD6 peaks (Figure 3B) in the C4-2 control cells. The nucleosome occupancy was increased significantly across the promoters of sharp CHD6 peaks compared with the promoters of broad CHD6 peaks (Figure S3B). High nucleosome occupancy is often associated with gene silencing and can affect gene expression levels, thereby influencing the cell function.[51] H3K9me3 and H3K27me3, as common repressive histone modifications,[52,53] exhibited higher signals in gene bodies with sharp CHD6 peaks than in those with broad CHD6 peaks (Figures 3C and 3D). To further confirm the impact of nucleosome density on the expression levels of genes characterized by different CHD6 binding patterns, we performed fold change (FC) analyses of gene expression levels between CHD6 knockdown and control cells. The results revealed that CHD6 knockdown led to the downregulation of the expression levels of genes with broad peaks and to minimal or no change in the expression levels of genes with sharp peaks (Figure 3E). Moreover, nucleosome occupancy at CHD6 binding sites with sharp peaks showed no change in response to CHD6 knockdown (Figure 3F), while significant alterations were observed across broad CHD6 peaks in promoter and gene body regions (Figure S3C). These observations suggest that CHD6 may regulate the density of nucleosomes at promoters, thereby controlling the low but stable expression levels of genes associated with sharp CHD6 peaks.

To further understand sharp CHD6 peaks beyond the C4-2 cell line, we collected RNA-seq data from normal (RWPE1, BPH1, and PrEC) and cancer cell lines (VCaP, LNCaP, 22RV1, PC3, and DU145) associated with the prostate. A significant decrease in expression level was observed in the genes with sharp CHD6 peaks compared with normal cell lines in most cancer cell lines (Figure 3G). Conversely, gene expression levels significantly increased in the genes with broad CHD6 peaks within the cancer cell lines compared with the normal cell lines (Figure S3D). Previous studies have suggested that the expression levels of HK genes undergo changes during the transition from normal to tumor cells.[30,31] Taking these data together, we conclude that genes characterized by sharp CHD6 peaks sustain low but stable expression levels, showing an expression pattern that is similar to that of HK genes.

Enriched motif of HK transcription factor in the genes with sharp CHD6 peaks

To examine the preferred binding motifs associated with distinct binding patterns of CHD6 and to elucidate the mechanisms involved in gene expression regulation, we performed a motif analysis on the regions associated with sharp and broad CHD6 peaks. We found that sharp CHD6 peaks were strongly enriched with the TFE3, USF2, USF1, and ETS1 motifs (Figure 4A), whereas broad CHD6 peaks were enriched with the ZNF711 and ZFX motifs (Figure 4B). TFE3 transcription factors belong to the microphthalmia family and are master regulators of organelle signaling, metabolism, and stress adaptation.[54] Previous studies have indicated that the functional domain of the TFE3 gene typically fuses with the promoter region of HK genes, which is a critical event for the occurrence of

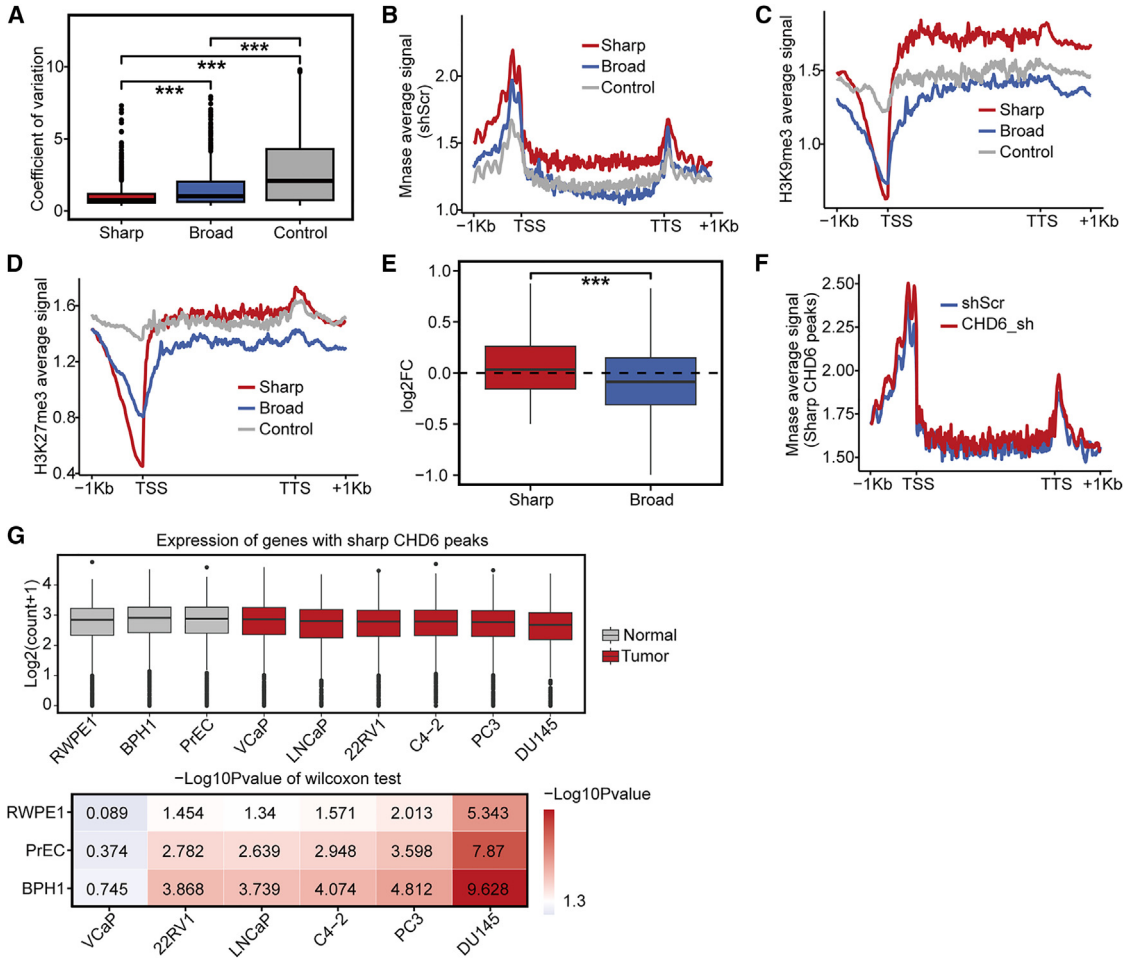

Figure 3. Expression levels of genes with sharp CHD6 peaks

(A) Coefficient of variation around groups. (B) Average MNase-seq read density plotted around genes. (C) Average ChIP-seq signal value of H3K9me3 plotted around genes. (D) Average ChIP-seq signal value of H3K27me3 plotted around genes. (E) The logFC (y axis) change in the genes with sharp and broad CHD6 peaks after CHD6 knockdown. (F) Nucleosome density of genes with sharp CHD6 peaks in both the C4-2 control cells and the CHD6 knockdown cells. (G) Comparison of gene expression levels between normal and cancer cell lines. *p* values determined using one-tailed Wilcoxon test. $^{*}p < 0.05$; $^{**}p < 0.01$; $^{***}p < 0.001$.

Xp11.2-translocation renal cell carcinoma.[55] USF2 and USF1 transcription factors, as determined by separate analyses using weight matrix collections of vertebrate transcription factor binding sites from TRANSFAC and PROMO, were predicted binding motifs that are overrepresented in HK gene promoters.[56] A previous study showed that ZNF711 may play a subordinate role in ZFX, which acts as a transcriptional activator in various types of human tumors.[57] These results indicate that the expression levels of genes with sharp CHD6 peaks are regulated by HK transcription factors.

To gain further support for the results that genes with sharp CHD6 peaks are regulated by the HK transcription factor, we collected ChIP-seq for ETS1 in the DU145 cell line. The distribution of all peaks represented the binding of ETS1 across the entire genome, indicating the regions where ETS1 interacted with the DNA. Among the total peaks, a notable enrichment in promoter regions is shown in the pie chart in Figure 4C. Consistent with our hypothesis, a striking 76% of the sharp CHD6 peaks were found to coincide with the regions where ETS1 binds in the promoter regions (Figure 4D). ETS1 and GABPA, both members of the ETS family transcription factor, were found to redundantly occupy promoters of HK genes in T cells.[58] The above studies indirectly suggested that the genes with sharp CHD6 peaks are associated with HK programs.

Sharp CHD6 marks HK genes in normal cells

Based on the results of the analysis of the genes with sharp CHD6 peaks in cancer cells, we supposed that sharp CHD6 peaks might also exist in normal cells. Therefore, we tested this hypothesis in two normal cells, HEK293 and cardiomyocytes. We observed remarkably consistent binding patterns of CHD6 in the normal cells resembling those observed in the cancer cells, which were characterized by high-density CHD6 peaks predominantly located on promoters,

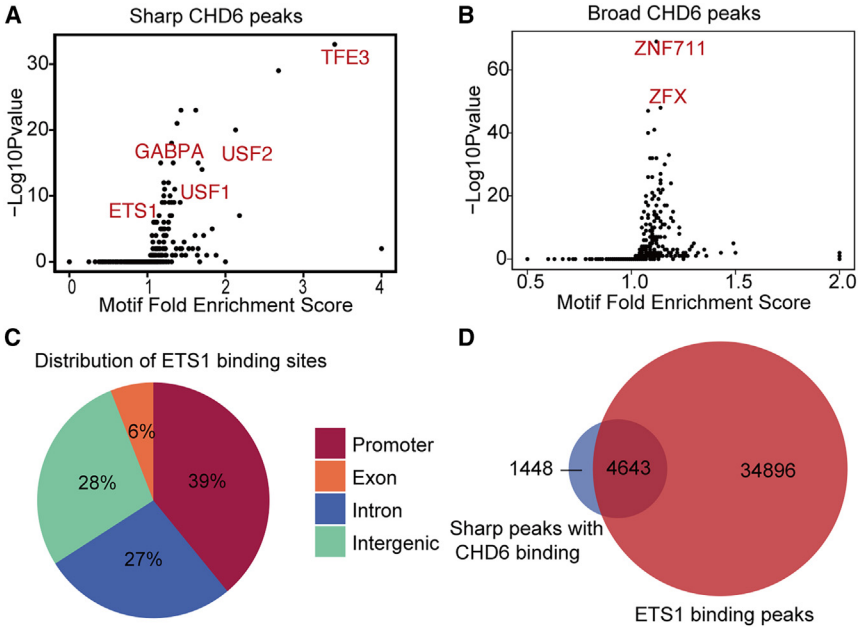

Figure 4. Characterization of sharp CHD6 peaks motifs and transcription factors

(A) Volcano plots of motif enrichment scores (percentage enrichment/percentage background) of the sharp CHD6 peaks compared with the log10 (*p* value). (B) Volcano plots of motif enrichment scores of the broad CHD6 peaks compared with the log10 (*p* value). (C) Distribution of ETS1 binding sites. (D) Venn diagram showing the overlap between the sharp CHD6 peaks and ETS1 binding peaks.

exhibiting narrow profiles. By contrast, the low-density CHD6 peaks were notably broader, spanning both promoter and gene body regions (Figure 5A). KEGG enrichment analysis revealed that pathways associated with mitophagy (hsa04137), autophagy (hsa04140) and apoptosis (hsa04210) were significantly enriched in the genes with sharp CHD6 peaks, but not in those with broad peaks or the control peaks (Figure 5B). The CHD6 peaks displaying sharp profiles in the promoter regions were found to be specifically enriched in HK genes, while lacking enrichment in OGs or TSGs (Figure 5C).

To determine whether the CHD6 binding pattern is conserved across different cell types, we identified 253 overlapping sharp CHD6 genes between HEK293 cells and cardiomyocytes (Table S2). These overlapping genes were significantly enriched in HK genes (Figure S4A). In addition, gene functional enrichment analysis using DAVID revealed strong associations with apoptosis and autophagy pathways (Figure S4B), which are both linked to HK processes. These findings provide compelling evidence that the observed pattern of sharp CHD6 peaks is closely linked to the HK regulatory network, a phenomenon consistently observed in both cancer and normal cells.

DISCUSSION

Chromatin remodelers are transcription regulators and play crucial roles in developmental processes.[59] Recent studies have indicated that developmental and HK gene transcription were regulated by distinct chromatin remodelers, highlighting the connection between chromatin structure and functional properties.[60] In this study, we have identified genes that characterize exclusive CHD6 binding at their promoter regions, namely sharp CHD6 peaks, which are preferentially enriched at HK genes within the C4-2 cell line. Our findings also show CHD6 binding in both the promoter and gene body regions of the genes, which suggests their potential as OGs, consistent with the findings of previous research.[24] The discovery of sharp CHD6 peaks, enriched at promoter regions of HK genes, implies the presence of a specialized regulatory mechanism that ensures the maintenance of essential cellular functions. Moreover, our results underscore the significance of CHD6 in prostate cancer progression, as evidenced by the differential expression levels of genes associated with sharp CHD6 peaks in cancer compared with normal prostate cells. Overall, our findings shed light on the role of CHD6 in modulating the expression levels of HK genes, thereby influencing fundamental cellular processes and potentially contributing to the rapid proliferation of cancer cells.

Different from broad CHD6 peaks, sharp CHD6 peaks are an indicator of decreased transcription elongation and enhancer inactivity. The distinct chromatin structure associated with sharp CHD6 peaks, which are characterized by increased nucleosome density and repressive histone modifications, suggests a mechanism for gene silencing and decreased transcriptional activity. In addition, the absence of significant enrichment in broad H3K4me3 modifications and SEs, which are characteristic of broad peaks, in sharp CHD6 peaks further supports the result of diminished enhancer activity. The lower levels of chromatin accessibility observed in sharp CHD6 peaks indicate a reduced activation state that may influence transcription machinery and gene expression.

Our study provides valuable insights into the regulatory role of CHD6 in PC, but our analysis focused primarily on coding genes, overlooking the potential regulatory roles of CHD6 in non-coding regions. In addition, beyond PC, we demonstrated the presence of a sharp CHD6 signature in the HK in normal cells. In future studies, we can further examine the potential regulatory role of CHD6 in noncoding regions and investigate its universality in other cancer types and normal tissues. This comprehensive investigation will deepen our understanding of how CHD6 regulates gene expression and tumor development.

In summary, our study emphasizes the role of sharp CHD6 peaks in maintaining the expression levels of HK genes, which are essential for sustaining life. Moreover, our findings elucidate the distinct CHD6 binding models involved in shaping the chromatin structure and

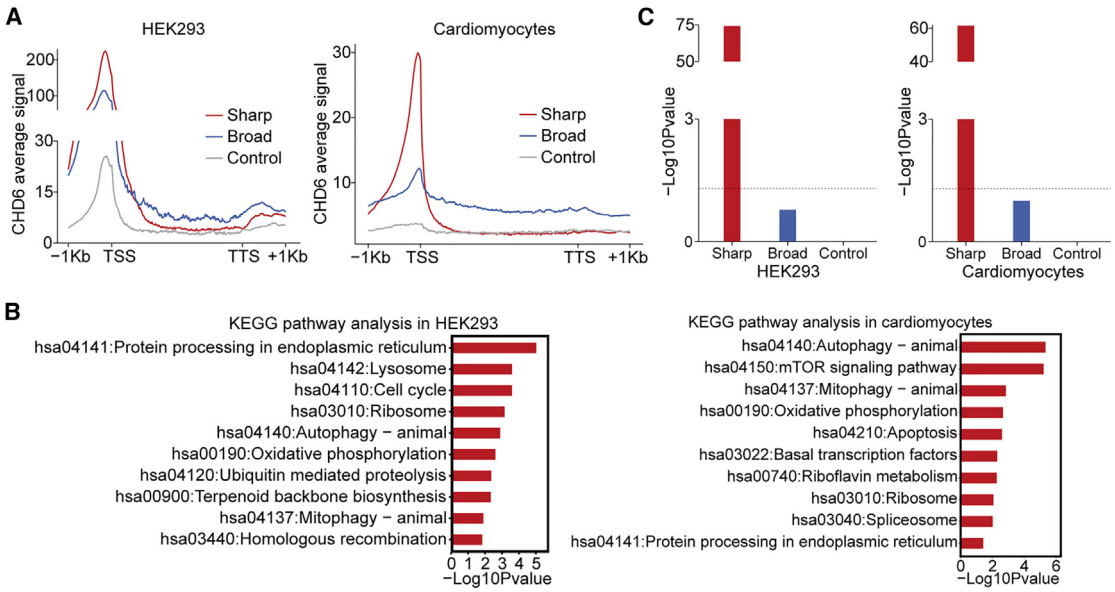

Figure 5. Characterization of genes with sharp CHD6 peaks in normal cells

(A) Average signal value of CHD6 peaks plotted around different genes in normal cells. (B) KEGG pathway enrichment of genes with sharp, broad, and control peaks in HEK293 and cardiomyocytes. (C) Enrichment *p* values (y axis) of the HK genes in HEK293 and cardiomyocytes. *p* values determined using Fisher's test exact test.

participating in various transcriptional programs. Overall, these findings deepen our understanding of the molecular mechanisms driven by CHD6, shedding light on essential cellular processes and their role in cancer or disease development. Importantly, they provide a foundation for future therapeutic interventions targeting chromatin remodelers in cancer treatment.

MATERIALS AND METHODS

Cell line and cell culture

The cell line HEK293 was purchased from the American Type Culture Collection and grown in DMEM complete medium with 10% fetal bovine serum. The cells were incubated at 37°C with 5% CO_2 and continuously cultured for less than 2 months. Cell lines were mycoplasma negative in routine tests.

Cleavage under targets and tagmentation

The cleavage under targets and tagmentation (CUT&Tag) assay (N259-YH01, Novoprotein Scientific) was performed in accordance with the manufacturer's instructions. Concanavalin A-conjugated magnetic beads were activated with binding buffer and incubated with washed cells. The cell-bead complex was incubated with antibodies, washed, and subjected to tagmentation with hyperactive pA-Tn5 transposase. After tagmentation, DNA was purified and libraries were prepared using the NovoNGS CUT&Tag 4.0 High-Sensitivity Kit. The libraries were then quantified and amplified. Sequencing was performed using Illumina NovaSeq PE150.

ChIP-seq analysis

ChIP-seq raw reads were mapped to the human genome version hg19 using Bowtie version 1.2.2 with default parameter values.[61] We then submitted the mapped reads to the Dpeak function in DANPOS version 2.2.2 (https://sites.google.com/site/danposdoc/) to calculate the ChIP-seq signal (read density) at each base pair of the genome,[62] subtract background (input) signal, normalize read number, and define individual enrichment peaks. The Dpeak stored the signal value at each base pair in a Wiggle format file, which we next converted to bigWig format using the tool wigToBigWig (https://www.encodeproject.org/software/wigtobigwig/). The Dpeak also stored individual feature values for each enrichment peak of the ChIP-seq signal. These feature values include peak width, height, and total signal. To calculate signal value at each base pair across each gene, we used the Profile function in DANPOS version 2.2.2. The Profile function in DANPOS 2.2.2 was also used to calculate the average ChIP-seq signal at each gene group. The colocalization of genomic loci was investigated with the Integrative Genomics Viewer.

CUT&Tag analysis

Approximately 1×10^5 cells were used for CHD6 (Bethyl, A301-221A) CUT&Tag assay. The raw sequencing image data were examined by the Illumina NovaSeq analysis pipeline. Before read mapping, clean reads were obtained from the raw reads by removing the adaptor sequences. The clean reads were then aligned to the unmasked human genome version hg19 using Bowtie2 version 2.4.5[63] and further analyzed by DANPOS version 2.2.2 (https://sites.google.com/site/danposdoc/).

RNA-seq and scRNA-seq analysis

RNA-seq raw reads were mapped to human genome version hg19 using TopHat version 2.1.1 with default parameter values.[61] The expression value (number of raw reads) for each gene was determined by the

software HTSeq version 0.9.1 with default parameter values.[61] Normalized (the trimmed mean of M-values method) expression values and differentially expressed genes were determined by edgeR version 3.10.5 run with an R version 3.2.1. We used the tool bedGraphToBigWig (https://www.encodeproject.org/software/bedgraphtobigwig/) to generate a bigWig file that contains RNA-seq signal (read density) at each base pair across the genome.

The scRNA-seq data on patients with PC were accessed in the NCBI GEO database under accession number GSE137829 and analyzed by Seurat (version 4.2.1) and an R toolkit (https://github.com/satijalab/seurat), using the software R (version 4.3.1). CopyKAT R package[64] is utilized to calculate single-cell copy-number profiles from 10× single-cell RNA data and predict tumor and normal cells.

MNase-seq analysis

MNase-seq raw reads were mapped to the human genome version hg19 using Bowtie version 1.2.2 with default parameter values.[61] We then submitted the mapped reads to the Dpos function (parameter: -smooth_width 0 -c 50000000 -u 1 -pheight 1e−200) in DANPOS version 2.2.2 (https://sites.google.com/site/danposdoc/) to calculate the MNase-seq signal (read density) at each base pair of the genome. The pipeline to observe the MNase-seq read density is the same as that described above for ChIP-seq. The Profile function in DANPOS version 2.2.2 was also used to calculate the average MNase-seq signal at each gene group.

Calculation of the RNA Pol II pausing index

We defined the pausing region as the region from 50 bp upstream to 300 bp downstream of the TSS and defined the elongation region as the region from 300 bp downstream of the TSS to 1 kb downstream of the TTS. We also normalized the read counts by the total number of mapped reads, presenting the results as reads per million. We then calculated the pausing index as the pausing-to-elongation ratio of RNA Pol II ChIP-seq read density.

Identification of SEs

SEs were identified using the ROSE tool.[65] Briefly, individual enhancers within 12.5 kb of one another were stitched together to form a single larger enhancer domain. Stitched enhancer domains were then ranked for input-normalized ChIP-seq occupancy of CHD6. The point on the x axis at which the tangent to a scaled graph with the x and y axes ranging from 0 to 1 that had a slope of 1 was used as a cutoff, above which stitched enhancers were classified as SEs.

Motif analysis

Motif enrichment analysis was performed using the findMotifsGenome.pl program in the HOMER software suite.[66]

Function enrichment analysis

Gene Ontology and KEGG pathway analyses were performed using the DAVID database version 6.8 (https://david.ncifcrf.gov). Pathways with p values smaller than 0.05 were defined as significantly enriched. Enrichment levels for HK genes, tumor suppressors, and OGs were defined based on Fisher's exact tests.

Statistical analysis

For bar plots and boxplots, p values were calculated using Wilcoxon's test and Fisher's exact test. Differences were considered significant when the p value was <0.05 ($^{*}p < 0.05$; $^{**}p < 0.01$; $^{***}p < 0.001$).

DATA AND CODE AVAILABILITY

The CUT&Tag sequencing data have been deposited to GEO (https://www.ncbi.nlm.nih.gov/geo/), with the accession number GSE264397. The RNA-seq, scRNA-seq, MNase-seq, H3K4me3, H3K4me1, H3K27ac, H3K9me3, and H3K27me3 ChIP-seq data for the cell types of prostate tissue were downloaded from the GEO database project website (https://www.ncbi.nlm.nih.gov/geo/). Table S1 contains all data information used in this study. All data are available in the article and its supplemental information.

ACKNOWLEDGMENTS

This work was supported by the National Key R&D Program of China (2021YFF1201100), the National Natural Science Foundation of China (32270603) and the Fundamental Research Funds for the Central Universities (BMU2021YJ057).

AUTHOR CONTRIBUTIONS

D.Z. and L.B.: conceptualization, resources, supervision, funding acquisition, methodology, and writing – review & editing. S.H.: data curation, data analysis, and writing – review & editing. Z.R. and C.W.: investigation, methodology, and software. B.-Y.S.: investigation and software. Y.L. and L.H.: methodology, validation, and experiments. All authors reviewed the results and approved the final version of the manuscript.

DECLARATION OF INTERESTS

The authors declare no conflicts of interest that pertain to this work.

SUPPLEMENTAL INFORMATION

Supplemental information can be found online at https://doi.org/10.1016/j.omtn.2024.102397.

REFERENCES

1. Bernal, A., Bechler, A.J., Mohan, K., Rizzino, A., and Mathew, G. (2024). The Current Therapeutic Landscape for Metastatic Prostate Cancer. Pharmaceuticals *17*, 351.
2. Sekhoacha, M., Riet, K., Motloung, P., Gumenku, L., Adegoke, A., and Mashele, S. (2022). Prostate Cancer Review: Genetics, Diagnosis, Treatment Options, and Alternative Approaches. Molecules *27*, 5730.
3. Braga-Basaria, M., Muller, D.C., Carducci, M.A., Dobs, A.S., and Basaria, S. (2006). Lipoprotein profile in men with prostate cancer undergoing androgen deprivation therapy. Int. J. Impot. Res. *18*, 494–498.
4. Rebello, R.J., Oing, C., Knudsen, K.E., Loeb, S., Johnson, D.C., Reiter, R.E., Gillessen, S., Van der Kwast, T., and Bristow, R.G. (2021). Prostate cancer. Nat. Rev. Dis. Prim. *7*, 9.
5. Tyagi, M., Imam, N., Verma, K., and Patel, A.K. (2016). Chromatin remodelers: We are the drivers. Nucleus *7*, 388–404.
6. Reyes, A.A., Marcum, R.D., and He, Y. (2021). Structure and Function of Chromatin Remodelers. J. Mol. Biol. *433*, 166929.
7. Centore, R.C., Sandoval, G.J., Soares, L.M.M., Kadoch, C., and Chan, H.M. (2020). Mammalian SWI/SNF Chromatin Remodeling Complexes: Emerging Mechanisms and Therapeutic Strategies. Trends Genet. *36*, 936–950.
8. Hankey, W., Chen, Z., and Wang, Q. (2020). Shaping Chromatin States in Prostate Cancer by Pioneer Transcription Factors. Cancer Res. *80*, 2427–2436.
9. Li, H., Gigi, L., and Zhao, D. (2023). CHD1, a multifaceted epigenetic remodeler in prostate cancer. Front. Oncol. *13*, 1123362.
10. Marfella, C.G.A., and Imbalzano, A.N. (2007). The Chd family of chromatin remodelers. Mutat. Res. *618*, 30–40.

11. Sims, R.J., Chen, C.F., Santos-Rosa, H., Kouzarides, T., Patel, S.S., and Reinberg, D. (2005). Human but not yeast CHD1 binds directly and selectively to histone H3 methylated at lysine 4 via its tandem chromodomains. J. Biol. Chem. *280*, 41789–41792.

12. Flanagan, J.F., Mi, L.Z., Chruszcz, M., Cymborowski, M., Clines, K.L., Kim, Y., Minor, W., Rastinejad, F., and Khorasanizadeh, S. (2005). Double chromodomains cooperate to recognize the methylated histone H3 tail. Nature *438*, 1181–1185.

13. Flanagan, J.F., Blus, B.J., Kim, D., Clines, K.L., Rastinejad, F., and Khorasanizadeh, S. (2007). Molecular implications of evolutionary differences in CHD double chromodomains. J. Mol. Biol. *369*, 334–342.

14. Hauk, G., and Bowman, G.D. (2011). Structural insights into regulation and action of SWI2/SNF2 ATPases. Curr. Opin. Struct. Biol. *21*, 719–727.

15. Mills, A.A. (2017). The Chromodomain Helicase DNA-Binding Chromatin Remodelers: Family Traits that Protect from and Promote Cancer. Csh Perspect Med *7*, a026450.

16. Colbert, L.E., Petrova, A.V., Fisher, S.B., Pantazides, B.G., Madden, M.Z., Hardy, C.W., Warren, M.D., Pan, Y., Nagaraju, G.P., Liu, E.A., et al. (2014). CHD7 Expression Predicts Survival Outcomes in Patients with Resected Pancreatic Cancer. Cancer Res. *74*, 2677–2687.

17. Kim, M.S., Chung, N.G., Kang, M.R., Yoo, N.J., and Lee, S.H. (2011). Genetic and expressional alterations of genes in gastric and colorectal cancers. Histopathology *58*, 660–668.

18. Caldon, C.E., Sergio, C.M., Schütte, J., Boersma, M.N., Sutherland, R.L., Carroll, J.S., and Musgrove, E.A. (2009). Estrogen regulation of cyclin E2 requires cyclin D1 but not c-Myc. Mol. Cell Biol. *29*, 4623–4639.

19. Bagchi, A., Papazoglu, C., Wu, Y., Capurso, D., Brodt, M., Francis, D., Bredel, M., Vogel, H., and Mills, A.A. (2007). is a tumor suppressor at human. Cell *128*, 459–475.

20. March, H.N., Rust, A.G., Wright, N.A., ten Hoeve, J., de Ridder, J., Eldridge, M., van der Weyden, L., Berns, A., Gadiot, J., Uren, A., et al. (2011). Insertional mutagenesis identifies multiple networks of cooperating genes driving intestinal tumorigenesis. Nat. Genet. *43*, 1202–1209.

21. Moore, S., Berger, N.D., Luijsterburg, M.S., Piett, C.G., Stanley, F.K.T., Schräder, C.U., Fang, S., Chan, J.A., Schriemer, D.C., Nagel, Z.D., et al. (2019). The CHD6 chromatin remodeler is an oxidative DNA damage response factor. Nat. Commun. *10*, 241.

22. Kargapolova, Y., Rehimi, R., Kayserili, H., Brühl, J., Sofiadis, K., Zirkel, A., Palikyras, S., Mizi, A., Li, Y., Yigit, G., et al. (2021). Overarching control of autophagy and DNA damage response by CHD6 revealed by modeling a rare human pathology. Nat. Commun. *12*, 3014.

23. Zhang, B., Liu, Q., Wen, W., Gao, H., Wei, W., Tang, A., Qin, B., Lyu, H., Meng, X., Li, K., et al. (2022). The chromatin remodeler CHD6 promotes colorectal cancer development by regulating TMEM65-mediated mitochondrial dynamics via EGF and Wnt signaling. Cell Discov. *8*, 130.

24. Zhao, D., Zhang, M., Huang, S., Liu, Q., Zhu, S., Li, Y., Jiang, W., Kiss, D.L., Cao, Q., Zhang, L., and Chen, K. (2022). CHD6 promotes broad nucleosome eviction for transcriptional activation in prostate cancer cells. Nucleic Acids Res. *50*, 12186–12201.

25. Eisenberg, E., and Levanon, E.Y. (2013). Human housekeeping genes, revisited. Trends Genet. *29*, 569–574.

26. Zhu, J., He, F., Hu, S., and Yu, J. (2008). On the nature of human housekeeping genes. Trends Genet. *24*, 481–484.

27. de Kok, J.B., Roelofs, R.W., Giesendorf, B.A., Pennings, J.L., Waas, E.T., Feuth, T., Swinkels, D.W., and Span, P.N. (2005). Normalization of gene expression measurements in tumor tissues: comparison of 13 endogenous control genes. Lab. Invest. *85*, 154–159.

28. Lee, P.D., Sladek, R., Greenwood, C.M.T., and Hudson, T.J. (2002). Control genes and variability: Absence of ubiquitous reference transcripts in diverse mammalian expression studies. Genome Res. *12*, 292–297.

29. Barber, R.D., Harmer, D.W., Coleman, R.A., and Clark, B.J. (2005). GAPDH as a housekeeping gene: analysis of GAPDH mRNA expression in a panel of 72 human tissues. Physiol. Genom. *21*, 389–395.

30. Byun, J., Logothetis, C.J., and Gorlov, I.P. (2009). Housekeeping genes in prostate tumorigenesis. Int. J. Cancer *125*, 2603–2608.

31. Chang, Y.C., Ding, Y., Dong, L., Zhu, L.J., Jensen, R.V., and Hsiao, L.L. (2018). Differential expression patterns of housekeeping genes increase diagnostic and prognostic value in lung cancer. PeerJ *6*, e4719.

32. Gundu, C., Arruri, V.K., Yadav, P., Navik, U., Kumar, A., Amalkar, V.S., Vikram, A., and Gaddam, R.R. (2022). Dynamin-Independent Mechanisms of Endocytosis and Receptor Trafficking. Cells *11*, 2557.

33. Marx, V. (2015). Autophagy: eat thyself, sustain thyself. Nat. Methods *12*, 1121–1125.

34. Mo, Y., Wang, Y., Zhang, L., Yang, L., Zhou, M., Li, X., Li, Y., Li, G., Zeng, Z., Xiong, W., et al. (2019). The role of Wnt signaling pathway in tumor metabolic reprogramming. J. Cancer *10*, 3789–3797.

35. Lauberth, S.M., Nakayama, T., Wu, X., Ferris, A.L., Tang, Z., Hughes, S.H., and Roeder, R.G. (2013). H3K4me3 Interactions with TAF3 Regulate Preinitiation Complex Assembly and Selective Gene Activation. Cell *152*, 1021–1036.

36. Shilatifard, A. (2012). The COMPASS family of histone H3K4 methylases: mechanisms of regulation in development and disease pathogenesis. Annu. Rev. Biochem. *81*, 65–95.

37. Hu, S., Song, A., Peng, L., Tang, N., Qiao, Z., Wang, Z., Lan, F., and Chen, F.X. (2023). H3K4me2/3 modulate the stability of RNA polymerase II pausing. Cell Res. *33*, 403–406.

38. Wang, H., Fan, Z., Shliaha, P.V., Miele, M., Hendrickson, R.C., Jiang, X., and Helin, K. (2023). H3K4me3 regulates RNA polymerase II promoter-proximal pause-release. Nature *615*, 339–348.

39. Zhang, Z., Shi, L., Dawany, N., Kelsen, J., Petri, M.A., and Sullivan, K.E. (2016). H3K4 tri-methylation breadth at transcription start sites impacts the transcriptome of systemic lupus erythematosus. Clin. Epigenet. *8*, 14.

40. Collins, B.E., Sweatt, J.D., and Greer, C.B. (2019). Broad domains of histone 3 lysine 4 trimethylation are associated with transcriptional activation in CA1 neurons of the hippocampus during memory formation. Neurobiol. Learn. Mem. *161*, 149–157.

41. Park, S., Kim, G.W., Kwon, S.H., and Lee, J.S. (2020). Broad domains of histone H3 lysine 4 trimethylation in transcriptional regulation and disease. FEBS J. *287*, 2891–2902.

42. Sayed, D., He, M., Yang, Z., Lin, L., and Abdellatif, M. (2013). Transcriptional regulation patterns revealed by high resolution chromatin immunoprecipitation during cardiac hypertrophy. J. Biol. Chem. *288*, 2546–2558.

43. Xiao, C., Fan, T., Tian, H., Zheng, Y., Zhou, Z., Li, S., Li, C., and He, J. (2021). H3K36 trimethylation-mediated biological functions in cancer. Clin. Epigenet. *13*, 199.

44. Yu, S., Li, J., Ji, G., Ng, Z.L., Siew, J., Lo, W.N., Ye, Y., Chew, Y.Y., Long, Y.C., Zhang, W., et al. (2022). Npac Is A Co-factor of Histone H3K36me3 and Regulates Transcriptional Elongation in Mouse Embryonic Stem Cells. Dev. Reprod. Biol. *20*, 110–128.

45. Zhu, I., and Landsman, D. (2023). Clustered and diverse transcription factor binding underlies cell type specificity of enhancers for housekeeping genes. Genome Res. *33*, 1662–1672.

46. Beacon, T.H., Delcuve, G.P., López, C., Nardocci, G., Kovalchuk, I., van Wijnen, A.J., and Davie, J.R. (2021). The dynamic broad epigenetic (H3K4me3, H3K27ac) domain as a mark of essential genes. Clin. Epigenet. *13*, 138.

47. Hnisz, D., Abraham, B.J., Lee, T.I., Lau, A., Saint-André, V., Sigova, A.A., Hoke, H.A., and Young, R.A. (2013). Super-Enhancers in the Control of Cell Identity and Disease. Cell *155*, 934–947.

48. Hughes, A.L., Kelley, J.R., and Klose, R.J. (2020). Understanding the interplay between CpG island-associated gene promoters and H3K4 methylation. Bba-Gene Regul Mech *1863*, 194567.

49. Tian, H., He, Y., Xue, Y., and Gao, Y.Q. (2022). Expression regulation of genes is linked to their CpG density distributions around transcription start sites. Life Sci. Alliance *5*, e202101302.

50. Joshi, C.J., Ke, W., Drangowska-Way, A., O'Rourke, E.J., and Lewis, N.E. (2022). What are housekeeping genes? PLoS Comput. Biol. *18*, e1010295.

51. Hesson, L.B., Sloane, M.A., Wong, J.W., Nunez, A.C., Srivastava, S., Ng, B., Hawkins, N.J., Bourke, M.J., and Ward, R.L. (2014). Altered promoter nucleosome positioning is an early event in gene silencing. Epigenetics *9*, 1422–1430.

52. Kim, J., and Kim, H. (2012). Recruitment and biological consequences of histone modification of H3K27me3 and H3K9me3. ILAR J. *53*, 232–239.

53. Zhou, C., Halstead, M.M., Bonnet-Garnier, A., Schultz, R.M., and Ross, P.J. (2023). Histone remodeling reflects conserved mechanisms of bovine and human preimplantation development. EMBO Rep. *24*, e55726.

54. Slade, L., and Pulinilkunnil, T. (2017). The MiTF/TFE Family of Transcription Factors: Master Regulators of Organelle Signaling, Metabolism, and Stress Adaptation. Mol. Cancer Res. *15*, 1637–1643.

55. Zhuang, W., Dong, X., Wang, B., Liu, N., Guo, H., Zhang, C., and Gan, W. (2021). NRF-1 directly regulates TFE3 and promotes the proliferation of renal cancer cells. Oncol. Lett. *22*, 679.

56. Farré, D., Bellora, N., Mularoni, L., Messeguer, X., and Albà, M.M. (2007). Housekeeping genes tend to show reduced upstream sequence conservation. Genome Biol. *8*, 1–10.

57. Rhie, S.K., Yao, L., Luo, Z., Witt, H., Schreiner, S., Guo, Y., Perez, A.A., and Farnham, P.J. (2018). ZFX acts as a transcriptional activator in multiple types of human tumors by binding downstream from transcription start sites at the majority of CpG island promoters. Genome Res. *28*, 310–320.

58. Hollenhorst, P.C., Chandler, K.J., Poulsen, R.L., Johnson, W.E., Speck, N.A., and Graves, B.J. (2009). DNA specificity determinants associate with distinct transcription factor functions. PLoS Genet. *5*, e1000778.

59. Zhang, F.L., and Li, D.Q. (2022). Targeting Chromatin-Remodeling Factors in Cancer Cells: Promising Molecules in Cancer Therapy. Int. J. Mol. Sci. *23*, 12815.

60. Hendy, O., Serebreni, L., Bergauer, K., Muerdter, F., Huber, L., Nemcko, F., and Stark, A. (2022). Developmental and housekeeping transcriptional programs in require distinct chromatin remodelers. Mol. Cell *82*, 3598-+.

61. Trapnell, C., Roberts, A., Goff, L., Pertea, G., Kim, D., Kelley, D.R., Pimentel, H., Salzberg, S.L., Rinn, J.L., and Pachter, L. (2012). Differential gene and transcript expression analysis of RNA-seq experiments with TopHat and Cufflinks. Nat. Protoc. *7*, 562–578.

62. Chen, K., Xi, Y., Pan, X., Li, Z., Kaestner, K., Tyler, J., Dent, S., He, X., and Li, W. (2013). DANPOS: dynamic analysis of nucleosome position and occupancy by sequencing. Genome Res. *23*, 341–351.

63. Langmead, B., and Salzberg, S.L. (2012). Fast gapped-read alignment with Bowtie 2. Nat. Methods *9*, 357–359.

64. Gao, R., Bai, S., Henderson, Y.C., Lin, Y., Schalck, A., Yan, Y., Kumar, T., Hu, M., Sei, E., Davis, A., et al. (2021). Delineating copy number and clonal substructure in human tumors from single-cell transcriptomes. Nat. Biotechnol. *39*, 599–608.

65. Whyte, W.A., Orlando, D.A., Hnisz, D., Abraham, B.J., Lin, C.Y., Kagey, M.H., Rahl, P.B., Lee, T.I., and Young, R.A. (2013). Master transcription factors and mediator establish super-enhancers at key cell identity genes. Cell *153*, 307–319.

66. Heinz, S., Benner, C., Spann, N., Bertolino, E., Lin, Y.C., Laslo, P., Cheng, J.X., Murre, C., Singh, H., and Glass, C.K. (2010). Simple combinations of lineage-determining transcription factors prime cis-regulatory elements required for macrophage and B cell identities. Mol. Cell *38*, 576–589.

OMTN, Volume *35*

Supplemental information

CHD6 eviction of promoter nucleosomes maintains housekeeping transcriptional program in prostate cancer

Lina Bu, Shaodong Huang, Ziyan Rao, Chenyang Wu, Bryan-Yu Sun, Yanhua Liu, Lin He, and Dongyu Zhao

Table S1. Summary of available data used in the study.

Data name	Data type	Cell	Cell type	ID (GEO database)
HEK293	CUT&Tag	HEK293	Normal	GSE264397
HEK293	CUT&Tag	HEK293	Normal	GSE264397
HEK293	CUT&Tag	HEK293	Normal	GSE264397
Cardiomyocytes	ChIP-seq	Cardiomyocytes	Normal	GSE136057
Cardiomyocytes	ChIP-seq	Cardiomyocytes	Normal	GSE136057
Cardiomyocytes	ChIP-seq	Cardiomyocytes	Normal	GSE136057
Cardiomyocytes	ChIP-seq	Cardiomyocytes	Normal	GSE136057
PolII	ChIP-seq	C4-2	Cancer	GSE55615
H3K4me3	ChIP-seq	C4-2	Cancer	GSE55615
H3K4me1	ChIP-seq	C4-2	Cancer	GSE55615
H3K27ac	ChIP-seq	C4-2B	Cancer	GSE105424
H3K27ac	ChIP-seq	C4-2B	Cancer	GSE105424
H3K36me3	ChIP-seq	C4-2B	Cancer	GSE118629
H3K36me3	ChIP-seq	C4-2B	Cancer	GSE118629
H3K9me3	ChIP-seq	C4-2B	Cancer	GSE118629
H3K9me3	ChIP-seq	C4-2B	Cancer	GSE118629
H3K27me3	ChIP-seq	C4-2B	Cancer	GSE118629
H3K27me3	ChIP-seq	C4-2B	Cancer	GSE118629
MNase	MNase-seq	C4-2	Cancer	GSE214212
MNase	MNase-seq	C4-2	Cancer	GSE214212
MNase	MNase-seq	C4-2	Cancer	GSE214212
MNase	MNase-seq	C4-2	Cancer	GSE214212
MNase	MNase-seq	C4-2	Cancer	GSE214212
MNase	MNase-seq	C4-2	Cancer	GSE214212
ATAC	ATAC-seq	C4-2B	Cancer	GSE145409
BPH1	RNA-seq	BPH1	Normal	GSE210205
BPH1	RNA-seq	BPH1	Normal	GSE210205
BPH1	RNA-seq	BPH1	Normal	GSE210205
BPH1	RNA-seq	BPH1	Normal	GSE210205
PrEC	RNA-seq	PrEC	Normal	GSE70466
PrEC	RNA-seq	PrEC	Normal	GSE70466
PrEC	RNA-seq	PrEC	Normal	GSE70466
RWPE1	RNA-seq	RWPE1	Normal	GSE118629
RWPE1	RNA-seq	RWPE1	Normal	GSE118629
RWPE1	RNA-seq	RWPE1	Normal	GSE118629
DU145	RNA-seq	DU145	Cancer	GSE210205
DU145	RNA-seq	DU145	Cancer	GSE210205
DU145	RNA-seq	DU145	Cancer	GSE210205
DU145	RNA-seq	DU145	Cancer	GSE210205

PC3	RNA-seq	PC3	Cancer	GSE210205
PC3	RNA-seq	PC3	Cancer	GSE210205
PC3	RNA-seq	PC3	Cancer	GSE210205
PC3	RNA-seq	PC3	Cancer	GSE210205
22RV1	RNA-seq	22RV1	Cancer	GSE214585
22RV1	RNA-seq	22RV1	Cancer	GSE214585
22RV1	RNA-seq	22RV1	Cancer	GSE214585
22RV1	RNA-seq	22RV1	Cancer	GSE214585
LNcap	RNA-seq	LNcap	Cancer	GSE193468
LNcap	RNA-seq	LNcap	Cancer	GSE193468
LNcap	RNA-seq	LNcap	Cancer	GSE193468
LNcap	RNA-seq	LNcap	Cancer	GSE193468
LNcap	RNA-seq	LNcap	Cancer	GSE193468
LNcap	RNA-seq	LNcap	Cancer	GSE193468
LNcap	RNA-seq	LNcap	Cancer	GSE193468
LNcap	RNA-seq	LNcap	Cancer	GSE193468
LNcap	RNA-seq	LNcap	Cancer	GSE193468
LNcap	RNA-seq	LNcap	Cancer	GSE193468
LNcap	RNA-seq	LNcap	Cancer	GSE193468
LNcap	RNA-seq	LNcap	Cancer	GSE193468
VCaP	RNA-seq	VCaP	Cancer	GSE136272
VCaP	RNA-seq	VCaP	Cancer	GSE136272
VCaP	RNA-seq	VCaP	Cancer	GSE136272
C4-2	RNA-seq	C4-2	Cancer	GSE214212
C4-2	RNA-seq	C4-2	Cancer	GSE214212
C4-2	RNA-seq	C4-2	Cancer	GSE214212
CRPC	scRNA-seq	CRPC	Cancer	GSE137829
CRPC	scRNA-seq	CRPC	Cancer	GSE137829
CRPC	scRNA-seq	CRPC	Cancer	GSE137829
CRPC	scRNA-seq	CRPC	Cancer	GSE137829
CRPC	scRNA-seq	CRPC	Cancer	GSE137829
CRPC	scRNA-seq	CRPC	Cancer	GSE137829
CRPC	scRNA-seq	CRPC	Cancer	GSE137829
CRPC	scRNA-seq	CRPC	Cancer	GSE137829
CRPC	scRNA-seq	CRPC	Cancer	GSE137829
CRPC	scRNA-seq	CRPC	Cancer	GSE137829
CRPC	scRNA-seq	CRPC	Cancer	GSE137829
CRPC	scRNA-seq	CRPC	Cancer	GSE137829

Table S2. Overlapping genes with sharp CHD6 peaks between HEK293 and cardiomyocytes.

TMEM55B	MRPL54	ELK1	SGTA	ZFYVE16	CC2D1B
BLOC1S3	MLH1	ZNF345	RPS26	ATP6V0B	AP4M1
MRPS18B	SKA2	CAPN10	ATP6V1G1	WDR77	HSPA13
TRAPPC6A	ATP5G1	HSPA9	ARID4A	AATF	UBE2Q1
CALR	EXOC8	CDV3	SLC20A1	CNPY3	DNAJB9
ZBTB37	SERBP1	BUB3	DNAJC16	AHSA1	RMND1
CD164	THAP5	DUS3L	AP4B1	FBXO17	HSP90B1
ASNA1	PRR3	C1orf174	PNISR	SH2B3	ARPC5
USP5	BCLAF1	SFR1	PSMD10	NOL6	UBE2S
SRSF2	ATF2	DCLRE1B	YIF1A	COMMD4	HMGN4
NFKBIB	UBAP2L	TCEANC2	UBE4B	SNX12	THNSL1
ZNF687	CNOT1	UVRAG	M6PR	WDR3	ALDH6A1
GLA	CD3EAP	CEP95	SLC2A4	DCTPP1	SDR39U1
SNRPD2	GIPC1	C1orf43	GANC	S100A1	ILVBL
HNRNPH2	COX14	C7orf25	ZNF318	RRAGC	PIAS4
TRAF7	EPM2AIP1	FAM192A	VPS33A	PPP1R15B	BLOC1S1
MPND	OSGEP	POLR2A	DESI1	PRDX6	LAMP1
APEX1	PABPN1	HNRNPDL	LAMTOR4	DNAJC13	IMP4
ZNF576	YBX1	GLYR1	CSTB	PQBP1	DACT3
C5orf51	DOLK	FAM76A	RBM39	ALDH3A2	BAX
CATSPERD	HIST1H4H	RPL19	FOXM1	ZMAT5	TMEM185B
SWSAP1	RPS12	HMBOX1	RPS28	FAF1	PET100
QPCTL	CD2BP2	TSR3	TSNAX	NBR1	CENPL
CYB5D1	FNIP1	UQCR11	PMVK	TMEM59	FAM179B
C19orf47	HMGN1	CCDC151	RPL9	MDH1	SUPV3L1
SHPK	CDK5	KIAA1009	ZNF706	RPL39	ULK3
CCNYL1	CNPY4	GTF2F1	SOCS5	CCT8	ZNF526
WBP1	MBTD1	PHB	PHF5A	PRELID1	TMEM131
ORC6	KLRG1	WDR75	TMTC3	OTUD1	CHCHD4
RBM42	UVSSA	PSMB3	MTF1	MAX	RUVBL2
LIN37	HPS5	MIEN1	FAM168B	FGFR1OP2	PARP6
ZNF181	GTF2H1	NPAT	FEN1	RPAIN	TXLNG
IER5	ZNF865	SRSF1	RPA1	LCN12	ENKUR
UBTD1	C8orf44	TOP3A	EIF3A	EXOSC1	RPL23
RIBC1	KIF20A	SPAG5	UBE2C	NAGA	ZNF503
DXO	HNRNPD	SIRT1	POLE3	EME1	PRPF38A
ZBTB5	CREB3L4	MLX	PLEKHH3	C12orf49	ALOXE3
C6orf211	CCDC115	RELL1	UBL5	TIMM17B	MMS19
TMEM116	ETF1	AP5Z1	AKR7A2	NGRN	RNF41

TIA1	H2AFV	DERL3	RBM23	RBX1	MRPL55
NTHL1	ZFP91	USO1	PPIP5K2	HINFP	PPP1R3D
UROD	GK	G6PC3	WDR92	B3GALT6	SLC35A5
MYL12A					

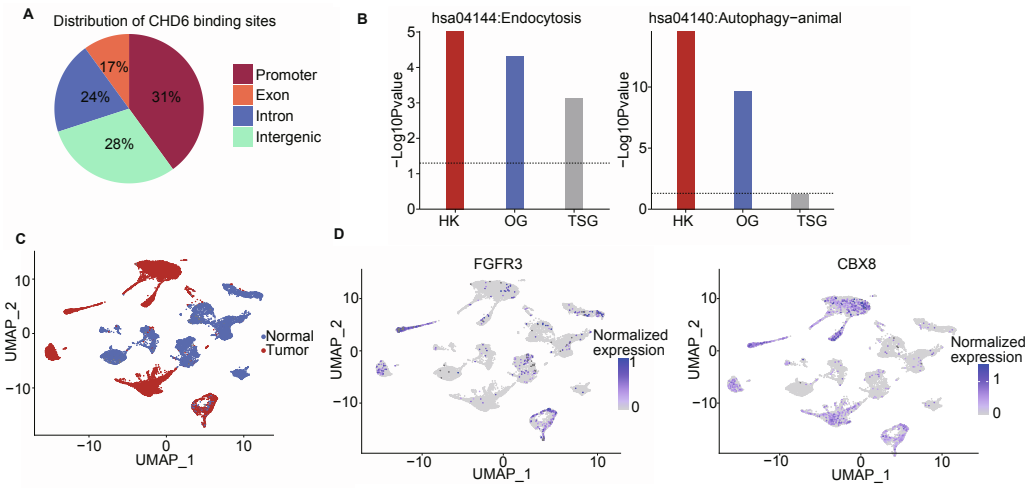

Figure S1. Distribution characteristics of the CHD6 binding sites.

(A) Distribution of CHD6 binding sites. (B) housekeeping genes (HK), oncogenes (OG) and tumor suppressors genes (TSG) are equally enriched in the KEGG pathways in endocytosis (left), and HK genes, and OG are equally enriched in the KEGG Pathways in autophagy-animal (right). (C) Distribution of tumor and normal cells using scRNA-seq. (D) Expression levels of the oncogene *FGFR3* and *CBX8* in tumor and normal cells. The P values determined using one tail Wilcoxon test.

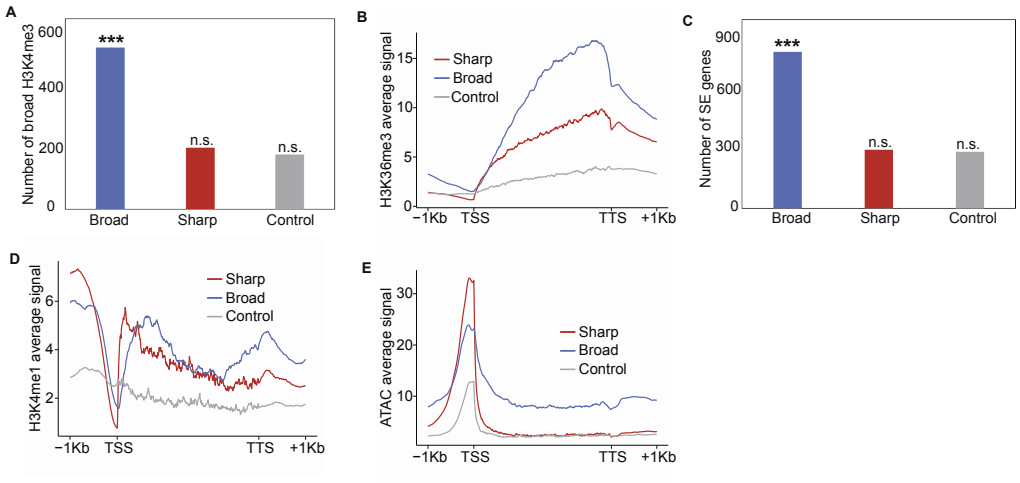

Figure S2. Binding models of CHD6 that differ in epigenetic modifications.

(A) Comparison of the overlap of different genes with broad H3K4me3. (B) Average ChIP-Seq signal value of H3K36me3 plotted around groups. (C) Comparison of the overlap of different genes with super enhancer genes. (D) Average ChIP-Seq signal value of H3K4me1 plotted around different genes. (E)Average ATAC signal value plotted around different groups. P values determined using one tail Wilcoxon test. *$p < 0.05$; **$p < 0.01$; ***$p < 0.001$. n.s., not significant.

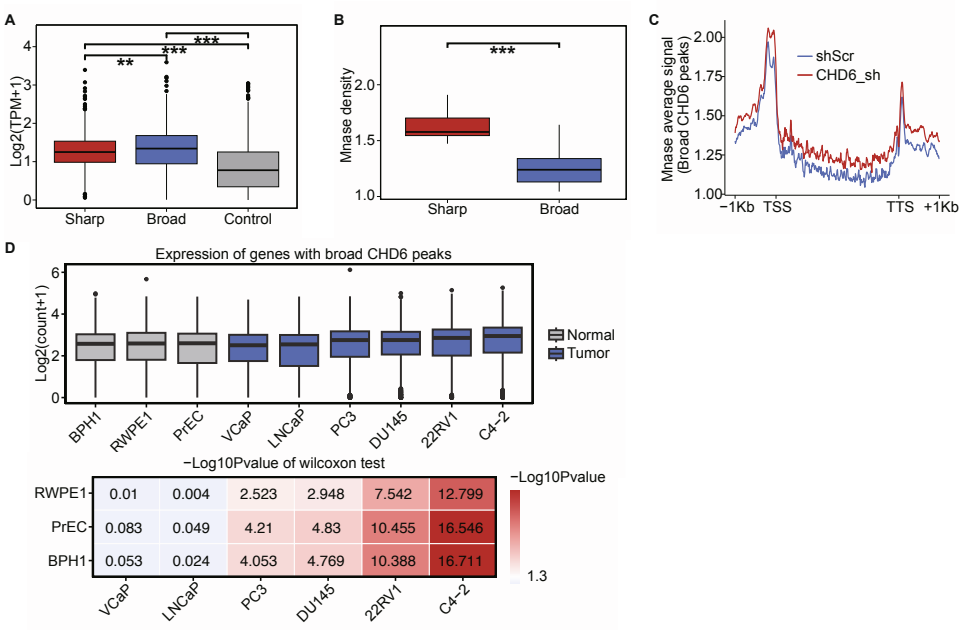

Figure S3. Higher nucleosome density of the genes with sharp CHD6 peaks than that of the genes with broad CHD6 peaks.

(A) Expression levels of genes determined from the GTEx tissue dataset. (B) The nucleosome density of the genes with sharp CHD6 peaks is significantly higher than those of the genes with broad CHD6 peaks. (C) Nucleosomes density of broad CHD6 peaks in both the C4-2 control cells and CHD6 knockdown cells. (D) Gene expression levels showing notable variations and significant differences between normal and cancer cell lines. P values determined using one tail Wilcoxon test. *$p < 0.05$; **$p < 0.01$; ***$p < 0.001$.

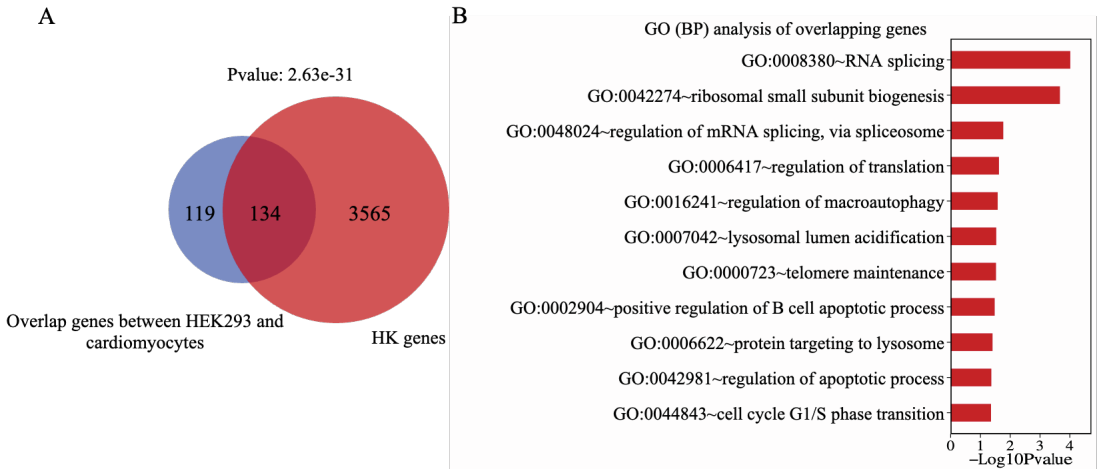

Figure S4. Detailed information on the overlap of genes with sharp CHD6 peaks between HEK293 and cardiomyocytes.

(A) Analysis of overlapping genes with enrichment in HK genes. (B) GO analysis of overlapping genes.